On the integral form of the motion equations for free surface flow

GIOVANNI CANNATA, CHIARA PETRELLI, LUCA BARSI, FLAMINIA CAMILLI, FRANCESCO GALLERANO
Department of Civil, Constructional and Environmental Engineering
"Sapienza" University of Rome
Via Eudossiana 18, 00184
ITALY
giovanni.cannata@uniroma1.it https://www.dicea.uniroma1.it/en/users/giovannicannata

Abstract: This work deals with a novel three-dimensional finite-volume non-hydrostatic shock-capturing model for the simulation of wave transformation processes and wave-structure interaction. The model is based on an integral formulation of the Navier-Stokes equations solved on a coordinate system in which the vertical coordinate is varying in time. A finite-volume shock-capturing numerical technique based on high order WENO reconstructions is adopted in order to discretize the fluid motion equations.

Key-Words: three-dimensional, time-dependent coordinate system, free surface flow, shock-capturing

1 Introduction

The modelling of surface wave transformation processes is crucial when dealing with the simulation of the hydrodynamic phenomena in coastal regions. Three-dimensional equations of motion can be used in order to represent most of these processes. In the most recent 3D models (Ma *et al.* [11]), the dynamic pressure is taken into account (free surface fully non-hydrostatic models). In such models, the total pressure is decomposed in its dynamic and hydrostatic parts. The solution of the fluid motion governing equations can be obtained as a succession of two different steps: in the first one, the convective terms are discretised together with those related to the hydrostatic pressure, the bottom slope and the stress term; in the second one, the so-called Poisson equation is solved in order to compute the dynamic pressure.

A way of solving the motion equations on domains which represent the complex physical geometry consists in transforming the complex computational domain in a regular domain. Such transformation can involve curvilinear coordinate systems which are time-dependent and moves with the free surface: the free surface and the bottom turn out always to be located respectively at the upper and the lower boundary of the computational domain. Moreover, the fluid pressure at the free surface is precisely set to zero, so that no approximation is involved in the assignation of the pressure condition at the upper boundary. In the work of Thomas and Lombard [13], the flow variables are represented by the Cartesian based velocity components multiplied by the Jacobian of the transformation.

The main difficulty in the simulation of the wave propagation from deep to shallow water (including the surf zone) is related to the approach adopted in order to reproduce the wave breaking. In this regard, an approach can be used based on the consideration that the wave breaking can be represented by the discontinuity of the weak solution of the integral form of the motion equations. The integral form of the motion equations, expressed in terms of conserved variables, allow high order shock-capturing numerical schemes to converge to correct weak solutions and, consequently, permit to directly simulate the breaking of the wave and the energy dissipation associated with it. In literature (Cannata *et al.* [2], Gallerano *et al.* [6], Shi *et al.* [12]), the motion equations are expressed in integral or differential conservative forms and in terms of conserved variables.

In the context defined by the simulation of free surface flows performed by using the motion equations in three-dimensional form integrated by methods of shock-capturing type, Weighted Essentially Non-Oscillatory (WENO) (Gallerano and Cannata [1], Jiang and Shu [8], Liu *et al.* [10], Gallerano *et al.* [4]) are often used, in which the numerical flux is approximated by using a convex combination of all candidate stencils. Liu *et al.* [10] proposed the cell-averaged version of the WENO scheme where a procedure by which the point values are reconstructed from the cell-averaged values is introduced. In this work, wave transformation is simulated by numerically solving the fluid motion equations written in a new integral form on a coordinate system in which the vertical coordinate is varying in time. The boundary conditions for pressure are placed on the upper face of each computational cell. The solution is advanced in time by using a three-stage Strong Stability Preserving Runge-Kutta (SSPRK) fractional step numerical method which is accurate to the third order, and at each stage a pressure correction formulation is

applied in order to get a fluid velocity field which is divergence-free. A shock-capturing technique based on high-order WENO reconstructions is employed in order to discretize the fluid motion equations. At every cell interface, the numerical flux is computed by solving an approximate HLL Riemann problem.

2 The Motion Equations In Time-Dependent Curvilinear Coordinate Systems

In integral form, the continuity and the momentum equations over a control volume $\Delta V(t)$ which varies in time read

$$\frac{d}{dt}\int_{\Delta V(t)} \rho dV + \int_{\Delta A(t)} \rho\left(u_m - v_m\right) n_m dA = 0 \tag{1}$$

$$\frac{d}{dt}\int_{\Delta V(t)} \rho u_l dV + \int_{\Delta A(t)} \rho u_l \left(u_m - v_m\right) n_m dA = \int_{\Delta V(t)} \rho f_l dV + \int_{\Delta A(t)} T_{lm} n_m dA \tag{2}$$

in which $\Delta A(t)$ is the control volume surface, $u_l\left(l=1,3\right)$ and $v_m\left(m=1,3\right)$ are respectively the velocity of the fluid and the velocity of the control volume surface, both defined in the Cartesian reference coordinate system $x^l\left(l=1,3\right)$ (in the present notation it is intended that the superscripts designate components instead of powers), $n_m\left(m=1,3\right)$ is the outward unit vector normal to the surface $\Delta A(t)$, ρ is the fluid density, T_{lm} is the stress tensor and $f_l\left(l=1,3\right)$ is the vector representing the unit mass body forces

$$f_l = -\frac{1}{\rho} p_{,l} - G\delta_{13} \tag{3}$$

where δ_{13} is the Kronecker delta and p is the total pressure (here the comma with an index in subscript denotes the derivative as $[\ ]_{,l} = \partial[\ ]/\partial x^l$). The total pressure is defined as the sum of its hydrostatic and dynamic components

$$p = \rho G\left(\eta - x^3\right) + q \tag{4}$$

in which G is the gravity constant, η is the elevation of the free surface and q is the dynamic pressure.

It is possible to rewrite the first integral on the right-hand side of Equation (2) in the following way

$$\int_{\Delta V(t)} \rho f_l dV = -\int_{\Delta V(t)} \left[\left(\rho G\eta + q\right)_{,l}\right] dV \tag{5}$$

The application of the Green's theorem makes it possible to rewrite the integral on the right-hand side of Equation (5) as follows

$$-\int_{\Delta V(t)} \left[\left(\rho G\eta + q\right)_{,l}\right] dV = -\int_{\Delta A(t)} \rho G\eta n_l \, dA - \int_{\Delta V(t)} \left[q_{,l}\right] dV \tag{6}$$

The introduction of Equation (6) into Equation (2) allows us to obtain

$$\frac{d}{dt}\int_{\Delta V(t)} \rho u_l dV = -\int_{\Delta A(t)} \left[\rho u_l \left(u_m - v_m\right) n_m + \rho G\eta n_l\right] dA - \int_{\Delta V(t)} \left[q_{,l}\right] dV + \int_{\Delta A(t)} T_{lm} n_m dA \tag{7}$$

Equation (7), in which the only external body force is given by the gravitational force, becomes in the case of an incompressible fluid

$$\frac{d}{dt}\int_{\Delta V(t)} u_l dV = -\int_{\Delta A(t)} \left[u_l \left(u_m - v_m\right) n_m + G\eta n_l\right] dA - \frac{1}{\rho}\int_{\Delta V(t)} \left[q_{,l}\right] dV + \frac{1}{\rho}\int_{\Delta A(t)} T_{lm} n_m dA \tag{8}$$

The first, the second and the third integral on the right-hand side of Equation (8) are respectively related to the convective term and the gradient of the hydrostatic pressure, the gradient of the dynamic pressure and the stress tensor.

For the purpose of simulating the fully dispersive wave phenomena, Equation (8) can be transformed as follows. Let $H(x^1,x^2,t) = h(x^1,x^2,t) + \eta(x^1,x^2,t)$ being h the still water depth. We aim to represent the geometry of the free surface and the bottom in an accurate way and to correctly assign on them the pressure and the kinematic conditions. Let (ξ^1,ξ^2,ξ^3,τ) be a curvilinear coordinate system which varies in time so as to follow the time variation of the free surface elevation; the following relations define the transformation from the Cartesian coordinates (x^1,x^2,x^3,t) to the curvilinear coordinates (ξ^1,ξ^2,ξ^3,τ)

$$\xi^1 = x^1 \qquad \xi^2 = x^2 \qquad \xi^3 = \frac{x^3 + h}{H} \qquad \tau = t \tag{9}$$

The following relation is also valid

$$v_3 = \frac{\partial x^3}{\partial \tau} \tag{10}$$

Basically, the coordinate transformation

described by Equation (9) is such that the time-dependent coordinates of the physical domain are mapped to a uniform transformed space where ξ^3 spans from 0 to 1.

Let $\vec{g}_{(l)} = \partial\vec{x}/\partial\xi^l$ and $\vec{g}^{(l)} = \partial\xi^l/\partial\vec{x}$ be respectively the covariant and the contravariant base vectors. The metric tensor is defined by $g_{(lm)} = \vec{g}_{(l)} \cdot \vec{g}_{(m)}$ and its inverse by $g^{(lm)} = \vec{g}^{(l)} \cdot \vec{g}^{(m)}$ $(l,m = 1,3)$ (Thompson *et al.* [14]). The Jacobian of the transformation is given by $\sqrt{g} = \sqrt{\det(g_{(lm)})}$. The transformation relations between vector $\vec{n}$ expressed in the Cartesian coordinate system and its contravariant and covariant components, $r^{(l)}$ and $r_{(l)}$, expressed in the curvilinear coordinate system are

$$r^{(l)} = \vec{g}^{(l)} \cdot \vec{n} \quad , \quad \vec{n} = r^{(l)} \vec{g}_{(l)}$$

$$r_{(l)} = \vec{g}_{(l)} \cdot \vec{n} \quad , \quad \vec{n} = r_{(l)} \vec{g}^{(l)} \tag{11}$$

These relations also apply to other vectors. It is not difficult to verify that, in the particular case of the above-mentioned transformation, $\sqrt{g} = H$.

We now introduce a restrictive condition on the control volume $\Delta V(t)$: in the following $\Delta V(t)$ must be considered as a volume element defined by surface elements bounded by curves lying on the coordinate lines. Let dA^α be the coordinate surface element on which the coordinate line ξ^α is constant, and $\vec{n}$ the unit vector defined in the Cartesian system of reference normal to the above surface element. Let us indicate with n_m and $g_m^{(\alpha)}$ respectively the *m*-th component (in the Cartesian reference system) of the unit vector $\vec{n}$ and the covariant base vector $\vec{g}^{(\alpha)}$. We have

$$n_m \, dA^\alpha = g_m^{(\alpha)} H d\xi^\beta d\xi^\gamma \tag{12}$$

Let us define the volume element in the physical space as $\Delta V(t) = \Delta x^1 \Delta x^2 \Delta x^3 = \sqrt{g}\Delta\xi^1\Delta\xi^2\Delta\xi^3$, and the volume element in the transformed space as $\Delta V^* = \Delta\xi^1\Delta\xi^2\Delta\xi^3$. It is not difficult to verify that the first one varies in time, whilst the second one is fixed in time. Similarly to what just made, it is possible to define the surface element in the physical and the transformed space respectively as $\Delta A(t) = \Delta x^\alpha \Delta x^\beta = \sqrt{g}\Delta\xi^\alpha\Delta\xi^\beta$ and $\Delta A^* = \Delta\xi^\alpha\Delta\xi^\beta$ (where $\alpha,\beta = 1,2,3$ are cyclic).

Let us also define the cell-averaged value of the primitive variables in the transformed space as

$$\overline{H} = \frac{1}{\Delta V^*}\int_{\Delta V^*} H d\xi^1 d\xi^2 d\xi^3$$

$$\overline{u_l} = \frac{1}{\Delta V^*}\int_{\Delta V^*} u_l d\xi^1 d\xi^2 d\xi^3 \tag{13}$$

and the cell-averaged value of the conserved variable as

$$\overline{Hu_l} = \frac{1}{\Delta V^*}\int_{\Delta V^*} Hu_l d\xi^1 d\xi^2 d\xi^3 \tag{14}$$

By using Equations (9), (12), (13) and (14), Equation (8) becomes

$$\begin{aligned}
\frac{\partial\overline{Hu}_l}{\partial\tau} = \frac{1}{\Delta V^*}\Bigg(& \\
& -\sum_{\alpha=1}^{3}\Bigg\{\int_{\Delta A^{*\alpha+}}\left[Hu_l\left(u_m - v_m\right)g_m^{(\alpha)} + GH^2 g_l^{(\alpha)}\right]d\xi^\beta d\xi^\gamma \\
& \qquad -\int_{\Delta A^{*\alpha-}}\left[Hu_l\left(u_m - v_m\right)g_m^{(\alpha)} + GH^2 g_l^{(\alpha)}\right]d\xi^\beta d\xi^\gamma\Bigg\} \\
& +\sum_{\alpha=1}^{3}\Bigg\{\int_{\Delta A^{*\alpha+}} GhHg_l^{(\alpha)} d\xi^\beta d\xi^\gamma \\
& \qquad -\int_{\Delta A^{*\alpha-}} GhHg_l^{(\alpha)} d\xi^\beta d\xi^\gamma\Bigg\} \\
& -\frac{1}{\rho}\int_{\Delta V^*}\frac{\partial q}{\partial\xi^k} g_l^{(k)} H d\xi^1 d\xi^2 d\xi^3 \\
& +\sum_{\alpha=1}^{3}\frac{1}{\rho}\Bigg\{\int_{\Delta A^{*\alpha+}} T_{lm} g_m^{(\alpha)} H d\xi^\beta d\xi^\gamma \\
& \qquad -\int_{\Delta A^{*\alpha-}} T_{lm} g_m^{(\alpha)} H d\xi^\beta d\xi^\gamma\Bigg\}\Bigg)
\end{aligned} \tag{15}$$

where $\Delta A^{*\alpha+}$ and $\Delta A^{*\alpha-}$ indicate the contour surfaces of the volume element on which ξ^α is constant and which are respectively located at the larger and the smaller value of ξ^α (here the indexes α,β and γ are cyclic). Equation (15) represents the integral form of the momentum equation, expressed in the time-dependent coordinate system (ξ^1,ξ^2,ξ^3,τ), with the velocities u_l and v_m defined in the Cartesian reference system. Since the integral on the left-hand side of Equation (8) depends on (ξ^1,ξ^2,ξ^3,τ), the related total time derivative has become a local time derivative in Equation (15). It can be noticed that the conserved variables are advanced in time within a transformed space which is not time-varying. The time variation of the geometric components is expressed by the time variation of the metric terms.

If the density ρ is uniform and constant, Equation (1) changes into

$$\frac{d}{d\tau}\int_{\Delta V^*} H d\xi^1 d\xi^2 d\xi^3 + \sum_{\alpha=1}^{3}\left\{\int_{\Delta A^{*\alpha+}}(u_m - v_m) g_m^{(\alpha)} H d\xi^\beta d\xi^\gamma - \int_{\Delta A^{*\alpha-}}(u_m - v_m) g_m^{(\alpha)} H d\xi^\beta d\xi^\gamma\right\} = 0 \quad (16)$$

which, by making explicit the summation over the index α, reads

$$\begin{aligned}&\frac{d}{d\tau}\int_{\Delta V^*} H d\xi^1 d\xi^2 d\xi^3 + \\ &\left\{\int_0^1\left[\int_{\xi^{1+}} Hu_1 d\xi^2\right]d\xi^3 - \int_0^1\left[\int_{\xi^{1-}} Hu_1 d\xi^2\right]d\xi^3\right\} \\ &+\left\{\int_0^1\left[\int_{\xi^{2+}} Hu_2 d\xi^1\right]d\xi^3 - \int_0^1\left[\int_{\xi^{2-}} Hu_2 d\xi^1\right]d\xi^3\right\} \\ &+\left\{\iint_{\Delta A^*_{xy}(\xi^3=1)}(u_m - v_m) g_m^{(3)} H d\xi^1 d\xi^2 \right. \\ &\left. - \iint_{\Delta A^*_{xy}(\xi^3=0)}(u_m - v_m) g_m^{(3)} H d\xi^1 d\xi^2\right\} = 0\end{aligned} \quad (17)$$

where $\Delta A^*_{xy} = \Delta\xi^1\Delta\xi^2$ is the horizontal surface element in the transformed space. If the surface and bottom kinematics boundary conditions are taken into account, the last bracket of Equation (17) vanishes. Furthermore, since ΔV^* is not time-varying and H does not depend on ξ^3 and bearing in mind that ξ^3 spans from 0 to 1, the following relation is valid

$$\begin{aligned}\frac{d}{d\tau}\int_{\Delta V^*} H d\xi^1 d\xi^2 d\xi^3 &= \int_0^1\left[\int_{\Delta A^*_{xy}}\frac{\partial H}{\partial\tau} d\xi^1 d\xi^2\right]d\xi^3 \\ &= \int_{\Delta A^*_{xy}}\frac{\partial H}{\partial\tau} d\xi^1 d\xi^2\end{aligned} \quad (18)$$

It is also possible to write

$$\frac{\partial\overline{H}}{\partial\tau} = \frac{1}{\Delta A^*_{xy}}\int_{\Delta A^*_{xy}}\frac{\partial H}{\partial\tau} d\xi^1 d\xi^2 \quad (19)$$

By applying the bottom and surface kinematic boundary conditions, by using Equations (13), (18) and (19) and by dividing Equation (17) by ΔA^*_{xy}, the following relation is obtained

$$\frac{\partial\overline{H}}{\partial\tau} + \frac{1}{\Delta A^*_{xy}}\int_0^1\sum_{\alpha=1}^{2}\left[\int_{\xi^{\alpha+}} Hu_\alpha d\xi^\beta - \int_{\xi^{\alpha-}} Hu_\alpha d\xi^\beta\right]d\xi^3 = 0 \quad (20)$$

in which $\xi^{\alpha+}$ and $\xi^{\alpha-}$ indicate the contour lines of the surface element ΔA^* on which ξ^α is constant and which are located at the larger and at the smaller value of ξ^α respectively. Equation (20) represents the equation which governs the motion of the free surface. Equations (15) and (20) represent the expressions of the three-dimensional equations of motion as a function of the $\overline{Hu_l}$ and $\overline{H}$ variables in the time-dependent coordinate system (ξ^1,ξ^2,ξ^3,τ). The simulation of the fully dispersive wave phenomena can be performed by numerically solving Equations (15) and (20). The Smagorinsky sub grid model is used in order to estimate the eddy viscosity in the stress tensor.

3 Numerical Scheme

Equations (15) and (20) are discretized by means of a combined finite-volume and finite-difference scheme with a Godunov-type method. A grid staggering is used where the fluid velocities are located at the centres of the computational cells and the fluid pressure is defined in correspondence of the horizontal faces of the cells. The discretization of the computational domain is based on a grid defined by the coordinate lines ξ^1, ξ^2 and ξ^3 and by the points of coordinates $\xi^1 = i\Delta\xi^1$, $\xi^2 = j\Delta\xi^2$ and $\xi^3 = k\Delta\xi^3$, which represent the centres of the calculation cells $I_{i,j,k} = (\xi^1_{i-1/2},\xi^1_{i-1/2})\times(\xi^2_{j-1/2},\xi^2_{j-1/2})\times(\xi^3_{k-1/2},\xi^3_{k-1/2})$. The state of the system is known at the computational cells centre and is identified by the cell-averaged values $\overline{Hu_l}$ and $\overline{H}$. The time level at which the variables are known is $\tau^{(n)}$, whilst the time level at which the variables are unknown is $\tau^{(n+1)}$.

A three-stage Strong Stability Preserving Runge-Kutta (SSPRK) scheme is used in order to solve Equations (15) and (20). With the purpose of getting a fluid velocity field which is divergence-free, a pressure correction formulation is adopted. Once $\overline{Hu_l}^{(n)}$ is known, the following three-stage iteration procedure is implemented in order to compute $\overline{Hu_l}^{(n+1)}$. Let

$$\overline{Hu_l}^{(0)} = \overline{Hu_l}^{(n)} \quad (21)$$

At every stage p (where $p = 1,2,3$), an auxiliary field $\overline{Hu_{l*}}^{(p)}$ is directly computed from Equations (15) by using the values obtained at the previous stage

$$\overline{Hu_{l*}}^{(p)} = \sum_{q=0}^{p-1}\left\{\Omega_{pq}\overline{Hu_l}^{(q)} + \Delta\tau\varphi_{pq} D\left[Hu_l^{(q)}, \tau^{(n)} + d_q\Delta\tau\right]\right\} \quad (22)$$

having indicated by $D(H,u_l,\tau)$ the right-hand side of Equations (15) devoid of the dynamic pressure gradient term. Further details on the calculation of

coefficients Ω_{pq}, φ_{pq} and d_q can be found in Gottlieb *et al.* [7]. The continuity equation is not satisfied by the auxiliary fluid velocity field $\bar{u}_{l*}^{(p)}$ (which is related to the auxiliary variable $\overline{Hu}_{l*}^{(p)}$ computed by Equation (22) starting from the value $\bar{H}_{*}^{(p-1)}$). For this reason, at every intermediate stage p the fluid velocity field and the fluid pressure field are corrected by means of a scalar potential Ψ which is computed by solving the well-known Poisson pressure equation. The latter equation reads as follows

$$\nabla^2\Psi^{(p)} = -\frac{\rho}{\Delta t}\nabla(\bar{u}_{l*}^{(p)}) \tag{23}$$

The irrotational corrector fluid velocity field is calculated by

$$\bar{u}_{1c}^{(p)} = \frac{\Delta t}{\rho}\left(\frac{\partial\Psi^{(p)}}{\partial\xi^1} + \frac{\partial\Psi^{(p)}}{\partial\xi^3}\frac{\partial\xi^3}{\partial x}\right)$$

$$\bar{u}_{2c}^{(p)} = \frac{\Delta t}{\rho}\left(\frac{\partial\Psi^{(p)}}{\partial\xi^2} + \frac{\partial\Psi^{(p)}}{\partial\xi^3}\frac{\partial\xi^3}{\partial y}\right) \tag{24}$$

$$\bar{u}_{3c}^{(p)} = \frac{\Delta t}{\rho}\left(\frac{\partial\Psi^{(p)}}{\partial\xi^3}\frac{\partial\xi^3}{\partial z}\right)$$

With the purpose of obtaining a non-hydrostatic, divergence-free fluid velocity field at every stage, the fluid velocity field itself has to be corrected in the following way

$$\bar{u}_{l}^{(p)} = \bar{u}_{l*}^{(p)} + \bar{u}_{lc}^{(p)} \tag{25}$$

Let us indicate with $L(H,u_l,\tau)$ the right-hand side of Equation (20). The depth $\bar{H}^{(p)}$ is advanced at the stage p as follows

$$\bar{H}^{(p)} = \bar{H}^{(p-1)} + L(\bar{H}^{(p-1)}, u_l^{(p-1)}, \tau^n + \Delta\tau) \tag{26}$$

The value of $\overline{Hu}_l^{(n+1)}$ is given by

$$\overline{Hu}_l^{(n+1)} = \overline{Hu}_l^{(3)} \tag{27}$$

In order to calculate the terms $D(H,u_l,\tau)$ and $L(H,u_l,\tau)$, the integrals on the right-hand side of Equations (15) and (20) are numerically approximated. The following sequence is implemented in order to perform the above calculation.

1. At the centre of the contour face which is common to two adjacent cells, two point values of the unknown variables are reconstructed by means of two WENO reconstruction defined on the two adjacent cells (Gallerano *et al.* [3]), starting from the cell averaged values.
2. The unknown variables at the contour faces centre are advanced in time by means of the solution of the HLL Riemann problem, in which the initial data are given by the above-mentioned two reconstructed values.
3. The spatial integrals involved in $D(H,u_l,\tau)$ and $L(H,u_l,\tau)$ are calculated by a high-order quadrature rule.
4. The Poisson pressure equation is solved by means of a four-colour Zebra line Gauss-Seidel alternate method in conjunction with a multigrid V-cycle technique.
5. The auxiliary velocity fields $\bar{u}_{l*}$ is corrected by means of the scalar potential Ψ.
6. The local total depth is advanced in time (Equation (20)) by means of the corrected divergence-free non-hydrostatic velocity field.

3.1 WENO reconstructions

With the purpose of explaining the WENO reconstruction technique implemented in this work, let us indicate by $(\bar{u}_l)_{i,j,k}$ the cell averaged values of the Cartesian velocity component u_l over the cell $I_{i,j,k}$. We also indicate by $(u)_{i+1/2,j,k}$ and $(u)_{i-1/2,j,k}$, respectively, the two point values of u_l at the centre of the faces over which the coordinate ξ^1 is constant and that are placed on the side of increasing and decreasing ξ^1 (an analogous notation is used the other cell faces). For the sake of brevity, we will only present the reconstruction technique of these point values. Three different steps are involved in this reconstruction:

- Step 1: Starting from the cell averages $(\bar{u}_l)_{i,j,k}$, reconstruction, along the coordinate ξ^3, of the surface averages $(\tilde{u}_l)_{i,j,k}$, that is defined by

$$(\tilde{u}_l)_{i,j,k} = \frac{1}{\Delta\xi^2}\int_{\xi^2_{j-1/2}}^{\xi^2_{j+1/2}}\left[\frac{1}{\Delta\xi^1}\int_{\xi^1_{i-1/2,}}^{\xi^1_{i+1/2,}} u_l(\xi^1,\xi^2,\xi^3)d\xi^1\right]d\xi^2 \tag{28}$$

- Step 2: Starting from the surface averages $(\tilde{u}_l)_{i,j,k}$, reconstruction, along the coordinate ξ^2, of the line averages, defined by

$$(\hat{u}_l)_{i,j,k} = \frac{1}{\Delta\xi^1} \int_{\xi^1_{i-1/2,}}^{\xi^1_{i+1/2,}} u_l(\xi^1, \xi^2, \xi^3) d\xi^1 \quad (29)$$

- Step 3: Starting from the line average $(\hat{u}_l)_{i,j,k}$, reconstruction, along the coordinate ξ^2, of the point values $(u)_{i+1/2,j,k}$ and $(u)_{i-1/2,j,k}$.

3.2 Numerical approximations of the spatial integrals

The numerical approximations of the double and triple integrals on the right-hand side of Equation (15) are obtained by adopting the procedure suggested in Gallerano *et al.* [5].

4 Results

In this section, the ability of the proposed model to simulate the vortices formation due to wave-structure interaction is demonstrated by simulating the passage of a solitary wave over a rigid rectangular submerged obstacle. The geometry of the test case consists of a 5m long rectangular channel in which the depth of the still water is 0.228m and a rectangular obstacle 0.114m high and 0.38m long is located at the bottom. A grid spacing of 0.0025m, a time step of 0.001s and 100 vertical layers are adopted. The numerical treatment of the obstacle problem is carried out by adopting the strategy proposed by Lin [9]. On the left boundary of the computational domain, the following equations are used in order to generate the solitary wave

$$\eta(t) = A \sec h^2 \left[\sqrt{\frac{3A}{4h^3}} C(t-T) \right] \quad (30)$$

$$u(t) = \frac{C\eta(t)}{h+\eta(t)} \quad (31)$$

where $A = 0.05m$ is the incident wave amplitude, h is the depth of the still water, $C = \sqrt{g(h+A)}$ is the celerity of the wave and $T = 1.0s$ is the time when the crest of the wave enters the domain.

Figures 1 to 5 show the fluid velocity field and the elevation of the free surface due to the wave-submerged obstacle interaction at different instants. As expected, vortical structures are generated both at the left and the right arris of the obstacle, coherently with Lin [9]. Figure 1 shows that, when the solitary wave approaches the rectangular obstacle, a small vortex is generated on the left corner of the obstacle. In the second of the considered instants (Fig. 2), the passage of the solitary wave produces an increase of the fluid velocity over the whole obstacle. When the peak of the solitary wave has reached the right arris of the rectangular obstacle, a second vortical formation begins to form behind this arris (Fig. 3). As shown in Figures 4 and 5, as the solitary wave propagates over the rectangular obstacle, the vortex formed at the left corner is stretched and the one formed at the right side grows in strength and size, in accordance with that observed by Lin [9].

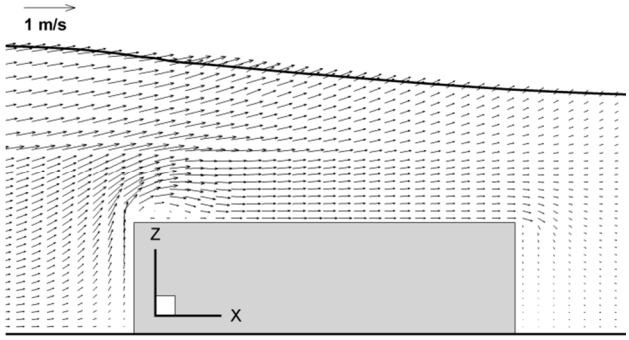

Fig. 1 Dynamics of the vortices generated by the wave-structure interaction. Fluid velocity field and elevation of the free surface at the instant $t = 2.42s$.

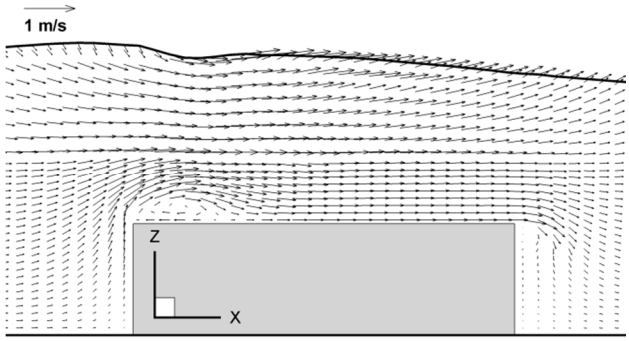

Fig. 2 Dynamics of the vortices generated by the wave-structure interaction. Fluid velocity field and elevation of the free surface at the instant $t = 2.62s$.

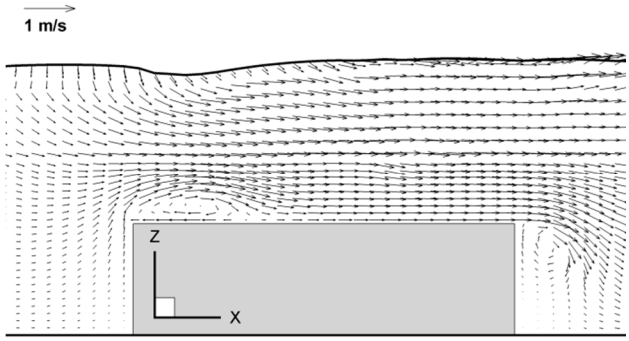

Fig. 3 Dynamics of the vortices generated by the wave-structure interaction. Fluid velocity field and elevation of the free surface at the instant $t = 2.80s$.

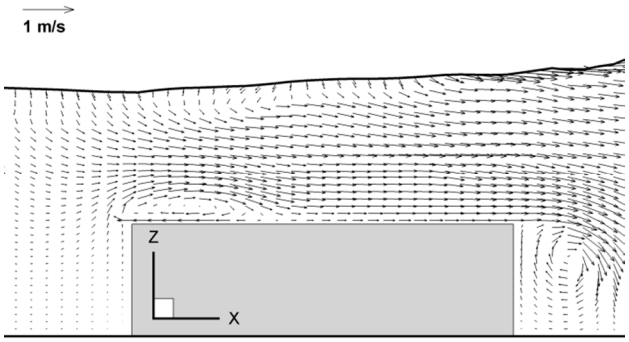

Fig. 4 Dynamics of the vortices generated by the wave-structure interaction. Fluid velocity field and elevation of the free surface at the instant $t = 2.98s$.

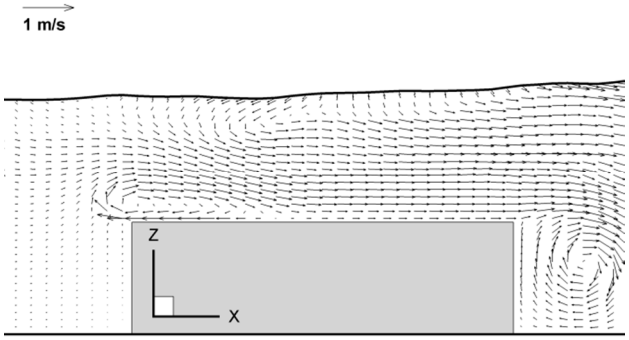

Fig. 5 Dynamics of the vortices generated by the wave-structure interaction. Fluid velocity field and elevation of the free surface at the instant $t = 3.12s$.

5 Conclusions

A new hydrodynamic model has been proposed which is based on an original integral formulation of the Navier-Stokes equations in a coordinate system in which the vertical coordinate is varying in time. The discretisation of the fluid motion equations is performed through a numerical technique which is based on high order WENO reconstructions. The time advancing of the solution is carried out by using a three-stage Strong Stability Preserving Runge-Kutta (SSPRK) fractional step numerical method which is accurate to the third order, and at each stage a pressure correction formulation is applied in order to get a fluid velocity field which is divergence-free. A shock-capturing technique based on high-order WENO reconstructions is employed in order to discretize the fluid motion equations. At every cell interface, the numerical flux is computed by solving an approximate HLL Riemann problem. As previously demonstrated the new finite-volume non-hydrostatic and shock-capturing three-dimensional model is able to simulate the vortices formation due to wave-structure interaction.

References:

[1] Gallerano F., Cannata G., Central WENO scheme for the integral form of contravariant shallow-water equations, *International Journal for Numerical Methods in Fluids*, 67, 2011, pp. 939-959.

[2] Cannata G., Lasaponara F., Gallerano F., Non-Linear Shallow Water Equations numerical integration on curvilinear boundary-conforming grids, *WSEAS Transactions on Fluid Mechanics*, 10, 2015, pp. 13-25.

[3] Gallerano F., Cannata G., Lasaponara F., A new numerical model for simulations of wave transformation, breaking and longshore currents in complex coastal regions, *International Journal for Numerical Methods in Fluids*, 80, 2015, pp. 571-613.

[4] Gallerano F., Cannata G., Lasaponara F., Numerical simulation of wave transformation, breaking run-up by a contravariant fully nonlinear Boussinesq model, *Journal of Hydrodynamics B*, 28, 2016, pp. 379-388.

[5] Gallerano F., Cannata G., Tamburrino M., Upwind WENO scheme for shallow water equations in contravariant formulation. *Computers & Fluids*, 62, 2012, pp. 1-12.

[6] Gallerano F., Cannata G., Villani M., An integral contravariant formulation of the fully nonlinear Boussinesq equations, *Coastal Engineering*, 83, 2014, pp. 119-136.

[7] Gottlieb S., Ketcheson D.I., Shu C.W., High order strong stability preserving time discretization, *Journal of Scientific Computing*, 38, 2009, pp. 251-289.

[8] Jiang G.S., Shu C.W., Efficient implementation of weighted ENO schemes, *Journal of Computational Physics*, 126, 1996, pp. 202-228.

[9] Lin P., A multiple layer σ-coordinate model for simulation of wave-structure interaction. *Computers & Fluids*, 35, 2006, pp. 147-167.

[10] Liu X.D., Osher S., Chan T., Weighted essentially non-oscillatory schemes, *Journal of Computational Physics*, 115, 1994, pp. 200-212.

[11] Ma G., Shi F., Kirby J.T., Shock-capturing non-hydrostatic model for fully dispersive surface wave processes, *Ocean Modeling*, 43-44, 2012, pp. 22-35.

[12] Shi F., Kirby J.T., Harris J.C., Geiman J.D., Grilli S.T., A high-order adaptive time-stepping TVD solver for Boussinesq modeling of breaking waves and coastal inundation. *Coastal Engineering*, 43-44, 2012, pp. 36-51.

[13] Thomas P.D., Lombard C.K., Geometric conservation law and its application to flow computations on moving grids, *AIAA Journal*, 17, 1979, pp. 1030-1037.

[14] Thompson J.F., Warsi Z.U.A., Mastin C.W., Numerical grid generation: foundations and applications, *Elsevier North-Holland, New York,* 198